SEISMIC REPAIR OF PRECAST RC BRIDGE COLUMNS CONNECTED WITH GROUTED SPLICE SLEEVES

Joel E. Parks, Dept. of Civil and Env. Engineering, University of Utah, Utah
Dylan N. Brown, Michael Baker International, Madison, WI
M.J. Ameli, Dept. of Civil and Env. Engineering, University of Utah, Utah
Chris P. Pantelides, PhD, PE, Dept. of Civil and Env. Eng., University of Utah, Utah

ABSTRACT

A repair technique for damaged precast reinforced concrete (RC) bridge columns with grouted splice sleeve (GSS) connections has been developed that utilizes a carbon fiber-reinforced polymer (CFRP) shell and epoxy anchored headed mild steel bars to relocate the column plastic hinge. Four original specimens were built using an Accelerated Bridge Construction (ABC) technique with two different GSS systems and were tested to failure using cyclic quasi-static loads. One GSS system was used to connect a precast RC bridge pier cap to a precast column and the second GSS system was used to connect a RC footing to a precast column, simulating an ABC bridge bent. Failure of the four original specimens occurred at drift ratios between 5.6% and 8.0% with longitudinal bar fracture or pullout from the GSS connections. The column plastic hinge region was repaired by increasing the column cross section from a 21 in. octagonal section to a 30 in. diameter circular section with an 18 in. height. The repair was constructed using a prefabricated CFRP shell, headed mild steel bars, and nonshrink or expansive concrete filling the void between the original columns and CFRP shell. The repair method successfully relocated the plastic hinge to the original column section adjacent to the repair and was capable of restoring the diminished load and displacement capacity. The method is a viable and cost-effective technique for rapid seismic repair of precast bridge assemblies.

Keywords: bridge; CFRP composite; column; repair; seismic; sleeve.

INTRODUCTION

Repair of severely damaged bridge elements following an earthquake is an advantageous alternative to replacement. The benefits include cost savings, reduction in construction time and decreased interruption of emergency services. The objective of bridge repair is to rehabilitate the damaged bridge elements to a performance level similar to the original performance by restoring the load and displacement capacity of the system. Capacity-based seismic design of bridges assigns damage to columns and protects the pier caps; hence, the paper is focused on column repair. Repair techniques for damaged bridge columns include the use of externally bonded Carbon Fiber-Reinforced Polymer (CFRP) jackets,[1-6] steel jackets[7-9] and concrete jackets.[10,11] However, until recently it has been assumed that when longitudinal bars within the column buckle or fracture the column should be replaced.[12]

Accelerated Bridge Construction (ABC) is gaining acceptance because of reduced construction time and minimal traffic interruption. Grouted Splice Sleeves (GSS) have been gaining attention as a possible precast concrete connection method for ABC in seismic regions. Current research is focused on the performance of GSS connections for bridges built in seismic regions.[13-16] The use of GSS connections in moderate to high seismic regions is imminent and a practical post-earthquake repair method is needed to accompany this new technology. Findings from current ABC research indicate that columns connected using GSS concentrate column damage and decrease the plastic hinge length compared to traditional monolithic construction.[17] These damage characteristics are advantageous for repair purposes, leaving a column section with minor damage for plastic hinge relocation.

The repair method developed has been designed and implemented on four severely damaged precast specimens connected using GSS. The original specimens had undergone quasi-static cyclic testing and had reached a severe damage state, before being repaired. The repair uses materials that are available and easy to install including epoxy anchored headed bars, CFRP sheets and nonshrink or expansive concrete.[18] The result is a cost effective, corrosion resistant, rapid repair procedure which could be installed in a few days. Due to the robust nature of the repair it is a suitable option for columns of varying damage states, including columns with buckled or fractured longitudinal bars.

EXPERIMENTAL INVESTIGATION OF ORIGINAL SPECIMENS

ORIGINAL TEST SPECIMENS

Four precast RC specimens representing half-scale bridge elements, conforming to current seismic bridge design standards, were constructed utilizing two different GSS systems.[19] Specimens NM-O1 and NM-O2 were column-to-footing assemblies connected using a GSS system which uses high strength nonshrink grout on both ends of the sleeve to splice the bars from the footing and column. Specimens LE-O1 and LE-O2 were column-to-pier cap assemblies connected using a GSS system which uses a threaded connection on one end of the sleeve and a grouted connection on the other. Nomenclature for the test specimens is as follows: the first two letters represent the splice sleeve type, GSS with both ends grouted =

NM and GSS with one end threaded and one grouted = LE; the letter “O” stands for original specimens and “R” stands for repaired specimen.

The geometry and reinforcement of the original specimens is shown in Fig. 1. The columns were 8.5 ft tall with a 21 in. wide octagonal cross section. The column longitudinal reinforcement consists of 6#8 grade 60 bars arranged in a circular pattern. The GSS connectors were located in the footing and pier cap for NM-O1 and LE-O1, respectively, and in the columns for NM-O2 and LE-O2. A #4 grade 60 spiral at a 2.5 in. pitch was provided for transverse column reinforcement. The footing was 6 ft long, 2 ft deep and 3 ft wide; the pier cap was 9 ft long, 2 ft deep and 2 ft wide. The material properties for the precast RC components and the repair are given in Table 1.

TESTING ASSEMBLY AND LOADING PROTOCOL

The test assembly, shown in Fig. 2(a), applied a lateral load at a point that represents the inflection point of an actual bridge column. The footing and pier cap have spans of 4 ft and 8 ft, respectively. The pier cap specimen was tested upside down, with the pier cap on the strong floor. Loading consisted of a constant axial load equal to 6% of the axial load capacity of the column and a displacement controlled cyclic quasi-static lateral load. The lateral load

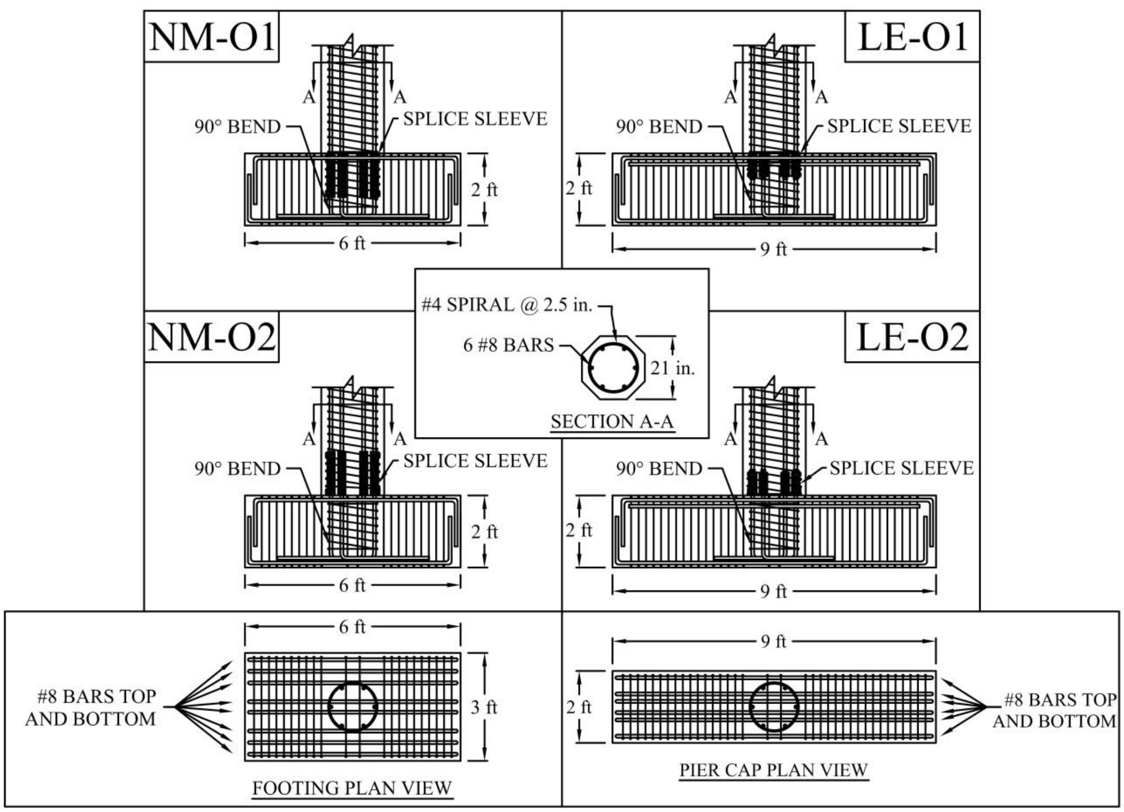

Figure 1. Original specimen reinforcement and geometry

Table 1. Material Properties

Material Properties		NM-O1	NM-R1	NM-O2	NM-R2	LE-O1	LE-R1	LE-O2	LE-R2
Longitudinal Bars	F_y, ksi (MPa)	68 (469)	68 (469)	68 (469)	68 (469)	68 (469)	68 (469)	75 (517)	75 (517)
	F_u, ksi (MPa)	93 (641)	93 (641)	93 (641)	93 (641)	93 (641)	93 (641)	103 (710)	103 (710)
Concrete Compresive Strength	Test-Day, ksi (MPa)	5.5 (38)	6.4 (44)	8.4 (58)	9.3 (64)	6.0 (41)	6.1 (42)	8.2 (57)	9.4 (65)

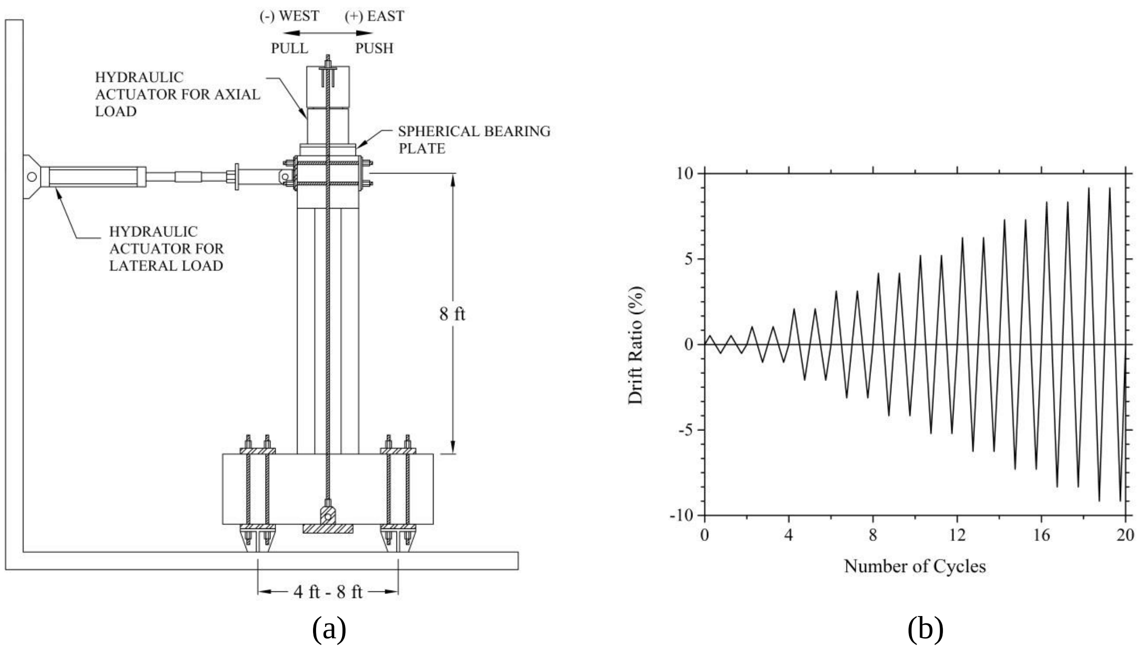

Figure 2. Test Assembly and Loading Protocol: (a) Test Assembly; (b) Loading Protocol.

was applied following the loading protocol shown in Fig. 2(b). Two cycles per drift ratio were used and the amplitude was progressively increased until a minimum 20% drop in the lateral load capacity was reached.[20] The drift ratio was taken in relation to the distance from the top of the footing or pier cap to the application of the lateral load.

ORIGINAL TEST SPECIMEN RESULTS

The damage state of the specimens prior to the repair is a critical parameter for the repair design and subsequent performance. The initial test results of NM-O1, NM-O2, LE-O1, and LE-O2 are summarized in Table 2 in terms of maximum lateral load, ultimate drift ratio, displacement ductility, reserve strength, and failure mode. The failure mode of NM-O1, NM-O2 and LE-O1 was fracture of an extreme longitudinal bar, while LE-O2 failed due to multiple longitudinal bars pulling out from the GSS connections in the column. The extreme east longitudinal bar fractured in both NM-O1 and NM-O2. The extreme west longitudinal bar fractured in LE-O1. At failure of all four original specimens, the lateral load capacity dropped well below 20% of the ultimate load. The reserve strength of the original columns after testing ranged from 44% to 65% of the lateral load capacity. A very well developed

Table 2. Original Specimen Test Results

Test Criteria	NM-O1	NM-O2	LE-O1	LE-O2
Lateral Load, kips (kN)	38.8 (173)	42.0 (187)	36.3 (161)	44.8 (199)
Ultimate Drift Ratio, %	6.69	7.91	6.50	6.00
Displacement Ductility	6.1	6.8	5.8	3.1
Reserve Strength, kips (kN)	21.4 (95)	23.6 (105)	20.6 (92)	15.9 (71)
Failure Mode	East Bar Fracture	East Bar Fracture	West Bar Fracture	Bar Pullout

plastic hinge formed at the footing-to-column and column-to-pier cap interfaces, as shown in Fig. 3. Extensive spalling and cracking occurred in the plastic hinge region of the original specimens. All original specimens experienced flexural cracking which extended 14 in. away from the footing or pier cap interface.

To assess the damage state of the original specimens a five-level performance evaluation approach was used.[21] This assessment procedure was based on the performance of the structure, which is defined by a particular damage state, and is classified into five levels. Level 1 is equivalent to no damage and level 5 is equivalent to local failure or collapse. According to this type of assessment the four original specimens had reached a damage state designation of level 5, since rebar fracture or pullout from the GSS occurred thus significantly compromising the lateral load carrying capacity of the columns. Structural components with a damage level of 5 usually require replacement. However, with the repair method developed in this research, repair of precast columns connected using GSS with level 5 damage is possible.

REPAIR DESIGN

The objective of the repair was to strengthen the original plastic hinge region by increasing the cross-section from a 21 in. octagonal cross-section to a 30 in. diameter circular cross-section. The 30 in. diameter circular cross-section was constructed by post-installing epoxy anchored headed bars for additional tensile reinforcement and then filling a CFRP shell with

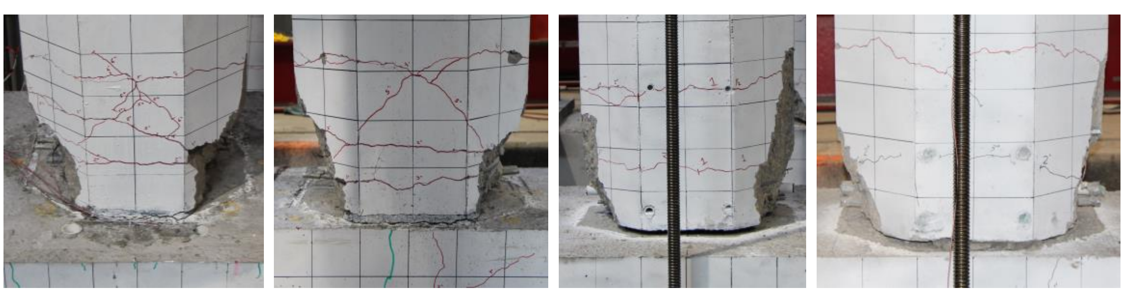

(a) (b) (c) (d)

Fig. 3–Original Specimen Damage: (a) NM-O1; (b) LE-O1; (c) NM-O2; (d) LE-O2.

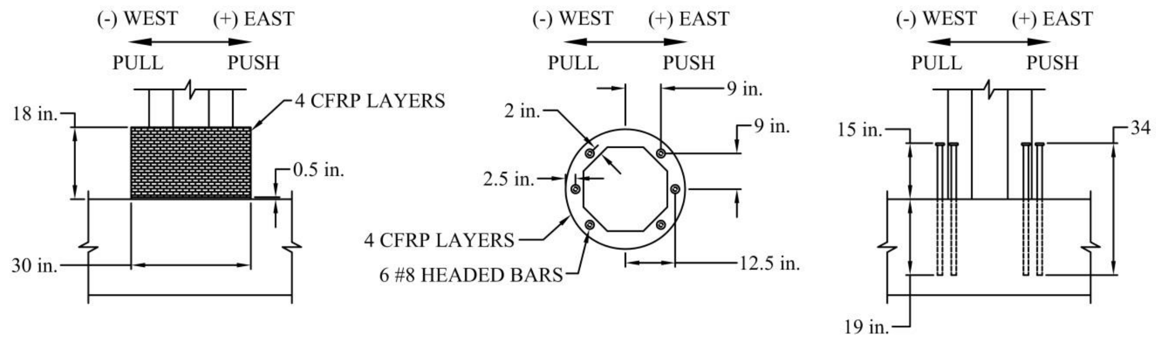

Figure 4. Repair design.

nonshrink or expansive concrete, as shown in Fig. 4. To form the new plastic hinge, a bending moment referred to as M_{PH} must be developed at the desired plastic hinge location. In the present case, the original specimen test results were used to determine M_{PH}; however, this bending moment can also be found using sectional analysis. From Fig. 5, the bending moment demand experienced at the column joint, M_{joint}, is a function of the length of the repair, H_{rep}, and the distance from the theoretical point of inflection to the column-footing or column-pier cap joint, H_{col}. This relationship is shown in Eq. (1).

$$M_{joint} = \frac{M_{PH}}{\left(1 - \frac{H_{rep}}{H_{col}}\right)} \tag{1}$$

Similar to the bending moment demand, the shear force demand that must be resisted by the column to achieve plastic hinge relocation, V_{PHR}, is directly related to H_{rep}. This relationship is shown in Eq. (2).

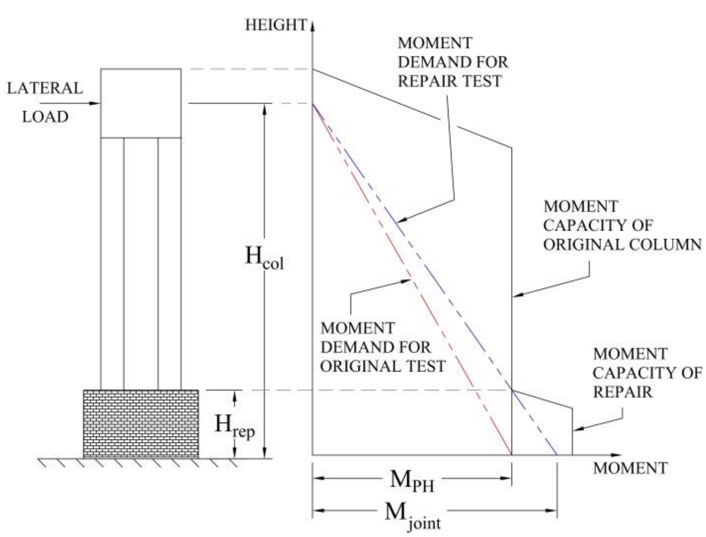

Figure 5. Bending moment demand.

$$V_{PHR} = \frac{M_{PH}}{(H_{col} - H_{rep})} \tag{2}$$

Eqs. (1) and (2) indicate that using the minimum possible repair height is advantageous for limiting the bending moment and shear demands. However, the height of the repair must be sufficient to relocate the new plastic hinge to a column cross-section which has only minor damage. From the observed damage of the four original specimens shown in Fig. 3, a repair height of 18 in. was determined to be sufficient. In this case there were two criteria to define the repair height. The first criterion was to relocate the plastic hinge above any structural cracks equal to or larger than 0.01 in. wide. The second was to provide enough height to develop the headed bars in tension.

Headed bars were designed to develop the increased joint bending moment, M_{joint}, required for the repair. The headed bar length drilled into the footing or pier cap was determined so that the epoxy anchorage would develop the bars in tension. Similarly, the length of headed bar extending into the repair was checked for adequate development length. These parameters led to the design of 6#8 grade 60 headed bars which were post installed around the column as shown in Fig. 4. Note that this is the same area of longitudinal reinforcement used for the original column design. The embedment into the footing or pier cap was 19 bar diameters and the length extending into the repair was 15 bar diameters. The headed bars used in this design had a head diameter of 2.25 in and a yield strength of 62 ksi.

The 30 in. diameter cross-section of the repair utilized a CFRP shell which was designed to provide concrete confinement, shear strength, and was also utilized as stay-in-place formwork for the nonshrink or expansive concrete. Four layers of unidirectional CFRP sheets oriented in the hoop direction were provided. One layer was provided to restore the shear strength of the original plastic hinge region; details of the design procedure are provided elsewhere.[22-24] Two layers were provided for confinement and prevention of strain softening and one layer was provided as the initial shell for wrapping subsequent CFRP layers. A 0.5 in. gap was left between the bottom of the jacket and footing or pier cap surface, as shown in Fig. 4, to ensure there was no bearing of the CFRP shell on the concrete during large displacements. The ultimate tensile capacity of the CFRP composite was 101 ksi [696 MPa], the modulus of elasticity was 8990 ksi [62000 MPa], and the ultimate strain was 1.12%, as determined by tensile coupon tests according to ASTM D3039.[25]

The shear capacity of the original column should be checked to ensure flexural failure at the location of the relocated plastic hinge. In this case, the transverse reinforcement in the relocated plastic hinge was sufficient to produce a flexural failure mode. If however, the shear capacity of the column was insufficient additional retrofit of the column would be necessary.

REPAIR PROCEDURE

Before beginning the repair the damaged columns were reset to the plumb position. Prefabricated CFRP shells were created by wrapping and curing a single layer of 18 in. wide

(a) (b) (c) (d)

Figure 6. Repair procedure: (a) post installed headed bars; (b) split CFRP shell; (c) CFRP shell around column; (d) CFRP shell filled with nonshrink or expansive concrete.

CFRP sheet around a 30 in. diameter sonotube to create the proper shape. While the CFRP shell was curing, the holes for the headed bars were core drilled into the footing or pier cap and the headed bars were epoxy anchored in-place, as shown in Fig. 6(a). After the CFRP shell had cured it was cut in two half cylinders and brought around the column as shown in Fig. 6(b). The sonotube inside the shell was used to ensure that the shell maintained its shape, while the additional layers of CFRP were applied and was subsequently removed once all CFRP layers had cured. A 12 in. long by 18 in. wide piece of CFRP sheet was used to splice the CFRP shell halves on both sides. Once the first layer of the CFRP shell was spliced, three additional CFRP layers were added as shown in Fig. 6(c). Each layer was 100 in. long by 18 in. wide, providing 6 in. overlap for each layer.

This was the last step in completing the construction of the CFRP shell which acted as stay-in-place formwork for the repair concrete. Once the CFRP shell had cured for 7 days, nonshrink or expansive concrete was added between the column and CFRP shell as shown in Fig. 6(d). The repair concrete had a compressive strength of 7.0 ksi.

For LE-O1 and LE-O2, the diameter of the repair was larger than the width of the pier cap. Wooden forms were placed alongside the pier cap to provide sufficient width for the repair as shown in Figs. 6(b) and 6(c). The wooden forms were removed once the concrete had cured. In practice, the pier cap would be oriented above the column and the gap between the repair and pier cap would provide an inlet for the concrete and the gap between the column and the repair would need to be sealed.

EXPERIMENTAL RESULTS FOR REPAIRED SPECIMENS

Since the damage state of all original specimens was similar, the same repair design was used for all specimens. The repair procedure was implemented for NM-O1, NM-O2, LE-O1 and LE-O2 and the repaired specimens are referred to as NM-R1, NM-R2, LE-R1 and LE-R2, respectively, where “R” stands for repaired specimen. The only difference in the repair was the type of concrete used to fill the void between the original column and CFRP shell. This concrete, referred to as the repair concrete, was nonshrink concrete for NM-R1 and LE-R1, and expansive concrete for NM-R2 and LE-R2. All test parameters for the repaired specimens are summarized in Table 3**.** The use of expansive instead of nonshrink concrete

Table 3. Repaired Specimen Test Parameters

Specimen ID	GSS Location	GSS Type	Repair Concrete
NM-R1	Footing	Grouted - Grouted	Nonshrink
NM-R2	Column	Grouted - Grouted	Expansive
LE-R1	Pier Cap	Fastened - Grouted	Nonshrink
LE-R2	Column	Fastened - Grouted	Expansive

converts the confinement provided by the CFRP shell from passive to active by pre-tensioning the CFRP shell.

The difference in active and passive confinement among the repaired specimens can be seen by the amount of pre-tensioning that was experienced by the CFRP wrap prior to testing. Strain gauges were used to monitor pre-tensioning for all repaired specimens. The magnitude of pre-tensioning is shown in Fig. 7. Specimens NM-R1 and LE-R1 designed with nonshrink concrete had low pre-tensioning between 0.016% and 0.015%, while specimens NM-R2 and LE-R2 designed with expansive concrete had significant pre-tensioning between 0.150% and 0.180%.

The test assembly and loading protocol were the same for the original and repaired specimens. The successful plastic hinge relocation of NM-R1 and LE-R1 is shown in Fig. 8. The strength and displacement capacity of the damaged bridge columns was restored for all repaired specimens.

SPECIMEN NM-R1

The hysteretic response of NM-R1 superimposed with the hysteretic response of NM-O1 is

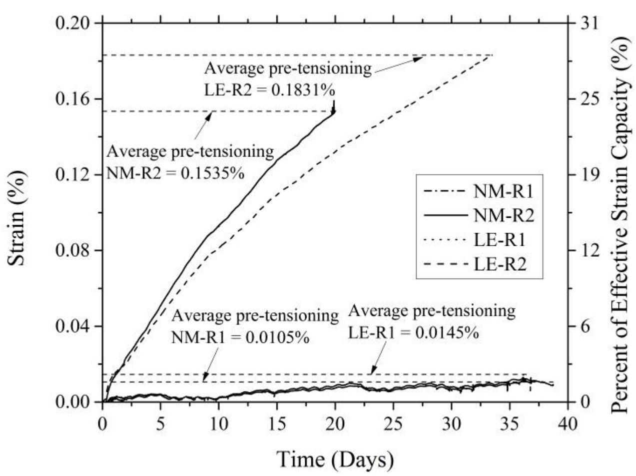

Figure 7. CFRP shell pre-tensioning.

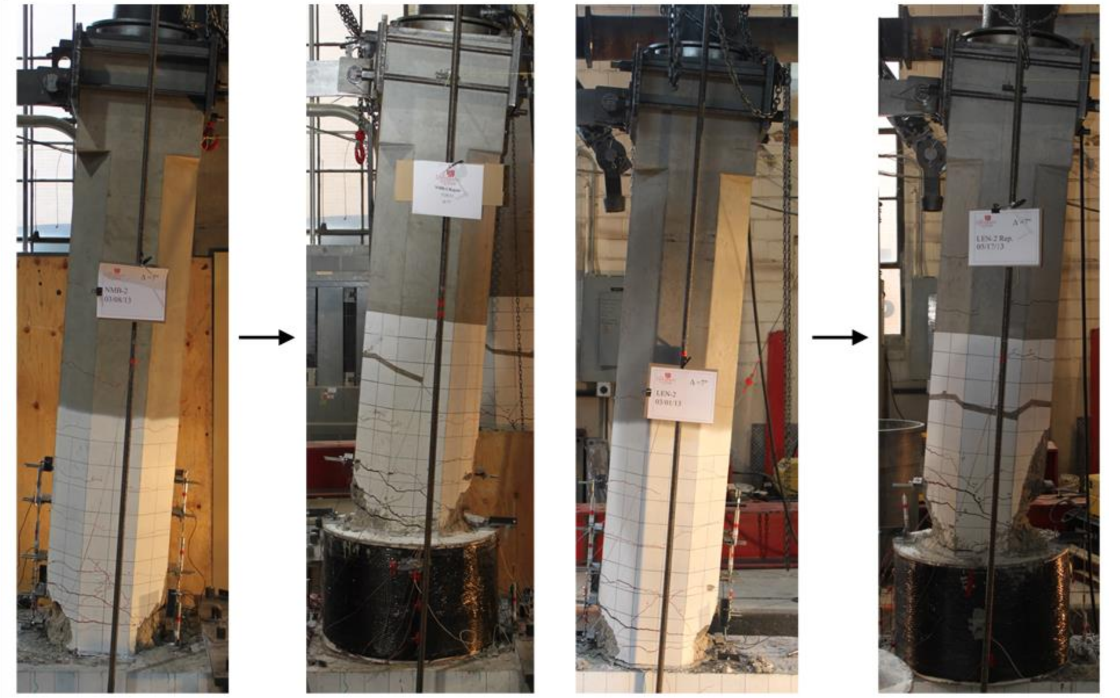

(a) (b) (c) (d)

Figure 8. Plastic hinge relocation: (a) NM-01; (b) NM-R1; (c) LE-01; (d) LE-R1.

shown in Fig. 9(a). From Fig. 9(a) and Table 4 it is clear that NM-R1 achieved a lateral load 18% higher than NM-O1 and had a similar displacement capacity. The failure mode of NM-R1 was fracture of column longitudinal bars in the relocated plastic hinge region. The extreme west longitudinal bar fractured during the first cycle of the 7.3% drift ratio and the extreme east longitudinal bar fractured during the second cycle of the same drift ratio. The east longitudinal bar fractured only 21.5 in. [546 mm] above the original fracture location in the original specimen NM-O1. This implies that the repair provided sufficient confinement and clamping force to develop the longitudinal bar in a short distance. Other major events included onset of significant spalling at a 3.1% drift ratio, and CFRP circumferential cracking in the fiber direction at a drift ratio of 4.2%. The CFRP crack was located approximately 3 in. [76 mm] below the top of the repair, at the same level as the top of the headed bars, and extended halfway around the jacket circumference on the east side. This is the same side the longitudinal column bar fractured in NM-O1. The hysteretic response of the specimen was unaffected by the circumferential crack in the CFRP shell.

SPECIMEN NM-R2

The hysteretic response of NM-R2 superimposed with that of NM-O2 is shown in Fig. 9(b).

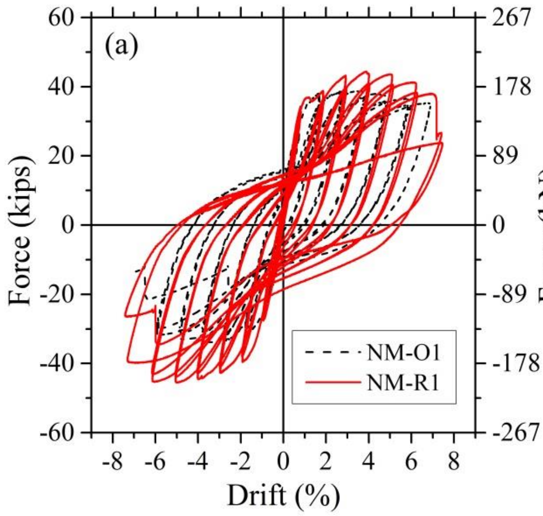

Figure 9. NM Hysteretic Response; (a) NM-R1 & NM-O1; (b) NM-R2 & NM-O2

Table 4. Repaired Specimen Test Results

Test Criteria	NM-R1	NM-R2	LE-R1 (Pushover)	LE-R1 (Cyclic)	LE-R2
Max Lateral Load, kips (kN)	45.6 (203)	53.6 (238)	46.8 (208)	40.5 (180)	50.5 (225)
Ultimate Drift Ratio, %	6.96	4.83	6.88	7.2	6.17
Displacement Ductility	6.0	3.7	6.6	---	4.6
Failure Mode	West & East Bar Fracture	West Bar Fracture	---	East Bar Fracture	CFRP Wrap Fracture

The failure mode of NM-R2 was fracture of the extreme west longitudinal bar during the 5.2% drift ratio. The lateral load capacity of NM-R2 was 28% higher than the lateral load capacity of NM-O2, as shown in Table 4. However, the displacement capacity of NM-R2 was less than that of NM-O2, at the ultimate displacement defined by a 20% drop in lateral load. The longitudinal column bar fracture, which caused the 20% drop in lateral load, was due to embrittlement from tack weld to hold instrumentation fixtures to the bar. The brittle fracture of the bar was obvious through several characteristics of the fracture. First, the fracture location was 10.5 in. above the top of the repair, which is significantly higher than the fracture location of all other tests which occurred within 5 in. of the column-repair interface; second, the fracture plane of the bar was smooth and level which is a characteristic of a brittle steel fracture plane; third, there was no decrease in diameter of the fractured bar when compared to the original diameter indicating no necking prior to the fracture.

Although a 20% drop in lateral load carrying capacity was observed, the test was carried out through the 8.3% drift ratio. The hysteretic response shows that despite the welding mishap, NM-R2 performed quite well in the west direction of testing after the column bar had fractured, outperforming NM-O2.

SPECIMEN LE-R1

In the case of specimen LE-R1, a monotonic pushover was performed along with the loading protocol of Fig. 2(b). The monotonic load was applied to the column in the east direction until a drift ratio of 6.9%. At this point, the column was brought back to its original vertical position and tested according to the loading protocol of Fig. 2(b). This series of loading emulates a near fault ground motion which is characterized by an acceleration pulse followed by sinusoidal ground motion.

The monotonic pushover curve is shown in Fig. 10(a). Although the column was displaced to a drift ratio beyond the ultimate drift ratio of LE-O1, no longitudinal bars fractured in the column due to the monotonic nature of the load. There was major spalling on the east side of the column, which can be seen in Fig. 8(d), that extended 20 in. up the column and exposed the spiral reinforcement.

With the repaired column already damaged in one direction from the monotonic pushover test, the specimen was subsequently tested cyclically. The hysteretic response of LE-R1 is shown in Fig. 10(a) superimposed with that of LE-O1. The right side of the hysteresis for LE-R1 shows an irregular response due to damage from the monotonic pushover. The left side of the hysteresis seems to be minimally affected; comparisons of the hysteretic response are made to this side of the hysteresis. The failure mode of LE-R1 was facture of the extreme east longitudinal bar in the relocated plastic hinge region. The bar fractured during the first cycle of the 7.3% drift ratio. Similar to the behavior of NM-R1, the onset of significant spalling on the west side of the column occurred at a 3.1% drift ratio and the onset of circumferential CFRP cracking occurred at a 4.2% drift ratio. Cracking was located approximately 3 in. below the top of the repair, at the top of the headed bars, and extended half way around the CFRP jacket circumference on the west side; this crack occurred on the same side as the longitudinal bar fracture in LE-O1. The specimen remained unaffected from the crack in the CFRP shell.

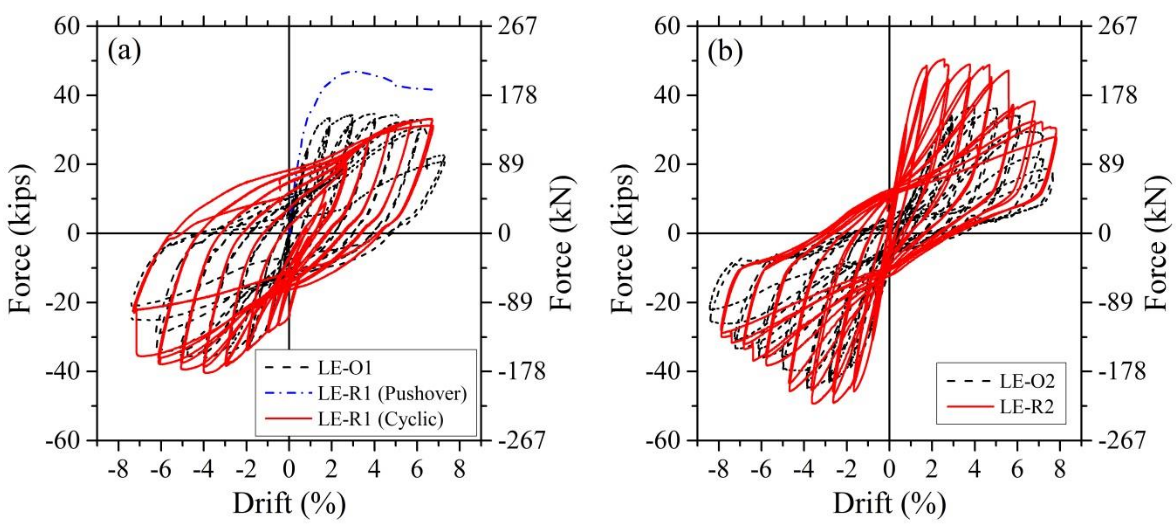

Figure 10. LE Hysteretic Response; (a) LE-R1 & LE-O1; (b) LE-R2 & LE-O2.

Due to the initial damage of LE-R1 from the monotonic pushover it is difficult to directly compare LE-R1 to LE-O1. However, by examining the performance of LE-R1 in Table 4 from both the monotonic pushover and cyclic tests, it is clear that LE-R1 performed similarly to LE-O1.

SPECIMEN LE-R2

The hysteretic response of LE-R2 superimposed with the hysteretic response of LE-O2 is shown in Fig. 10(b). During the 3.1% drift ratio a crack occurred and extended over the entire circumference of the CFRP shell, which correlated with the top of the headed bars. Failure of LE-O2 was due to pullout of the longitudinal column bars after yielding on both column sides; this caused additional demand on both sides of the repair causing the circumferential crack in the CFRP shell on both sides.

Before the plastic hinge was completely relocated above the repair, the CFRP shell fractured. Fracture of the CFRP shell occurred during the first cycle of the 6.3% drift ratio, which caused a 20% drop in the lateral load. This fracture occurred directly below the top of the headed bars and the circumferential CFRP crack on the north-east side of the repair. Although a 20% drop in lateral load carrying capacity was observed during the 6.3% drift ratio, the test was continued through the 8.3% drift ratio. As the test progressed, the CFRP jacket fractured three additional times, with each fracture moving closer to the column pier cap interface.

Despite the fact that the plastic hinge was not relocated entirely above the repaired region, the specimen still showed acceptable hysteretic performance. The lateral load capacity of LE-R2 was 13% higher than the lateral load capacity of LE-O2. However, once the CFRP jacket had fractured, the hysteretic response of LE-R2 followed closely the response of LE-O2.

The reasons for failure of LE-R2 in the CFRP shell rather than in the column cross-section adjacent to the repair are: (i) the GSS was located in the column leading to a different failure mode, which is pullout failure of the GSS rather than rebar fracture; as such, the plastic hinge in LE-O2 is shorter than when the sleeves were located in the pier cap as in LE-O1. With a shorter plastic hinge, damage does not spread up the column, implying that the repair could have been shorter, thus reducing the flexural demand in the repaired region; (ii) the strength of the column cross-section adjacent to the repair; by comparing material properties between LE-O1 and LE-O2 there was a 10% increase in the yield strength of the longitudinal bars and a 54% increase in the concrete compressive strength. The stronger column cross-section combined with minimal damage increased the required moment capacity to higher levels than expected, thus causing failure to occur. Both reasons relate to the original damage state of the column. Therefore, the importance of having a good assessment of the damaged column strength cannot be overstated.

PERFORMANCE OF THE REPAIRED SPECIMENS

Cumulative hysteretic energy dissipation and stiffness degradation characteristics of the NM specimens are compared in Figs. 11. Specimens LE-O1 and LE-R1 are omitted due to the monotonic test of LE-R1 which affects the cyclic performance. Specimens LE-O2 and LE-R2 are also omitted due to the pre-damaged nature of LE-O2, thus causing an inaccurate comparison.[17] The cumulative energy dissipation of NM-R1 and NM-R2 is greater than that of their original counterparts for all drift ratios. At completion of the 6.3% drift ratio, NM-R1 and NM-R2 dissipated 15% and 9% more energy than NM-O1 and NM-O2, respectively. Similarly, the stiffness degradation characteristics of NM-R1 and NM-R2 match those of NM-O1 and NM-O2, when normalized to the 0.5% drift ratio stiffness; the normalization was carried out to show stiffness degradation rather than numerical stiffness values, since the repaired specimens have a higher stiffness due to the shorter column length and higher column concrete compressive strength. Both cumulative energy dissipation and stiffness degradation characteristics of the repaired specimens further confirm that the repair can restore the assembly to a performance level similar to the original condition.

Table 4 shows the test results for all repaired specimens. When these results are compared to Table 2 for the original specimens, it can be observed that the repaired specimens were able to regain the strength achieved by the original specimens while still performing in a ductile manner in all cases.

CONCLUSIONS

A repair procedure for post-earthquake damage has been developed for severely damaged precast bridge columns connected using GSS connectors located in the column, footing, or pier cap. The repair converts the original plastic hinge region of an octagonal column to a larger circular cross section, thereby relocating the new plastic hinge to a section adjacent to the repair. This repair procedure was implemented for damaged precast bridge column-to-footing and column-to-pier cap assemblies which were tested under quasi-static cyclic loads.

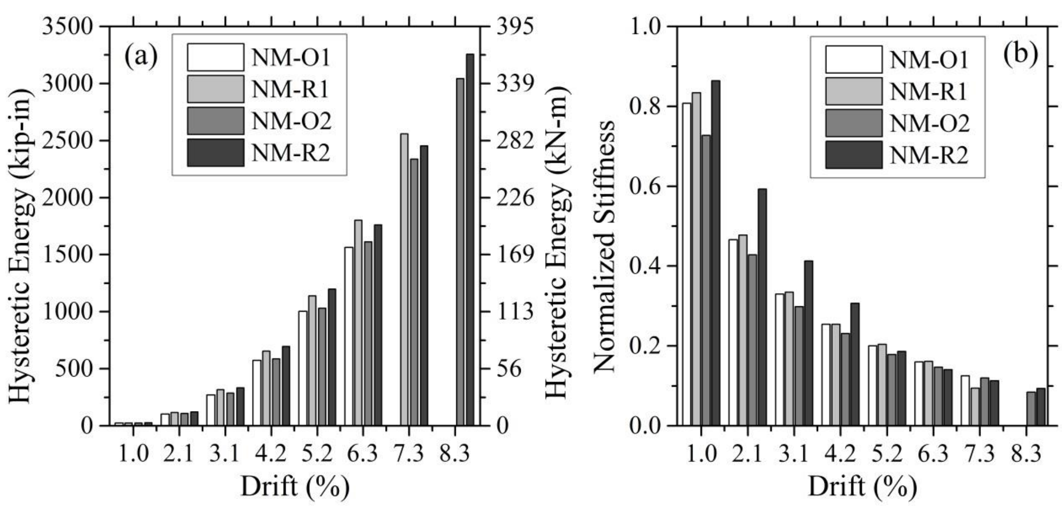

Figure 11. System performance: (a) cumulative energy dissipation; (b) normalized stiffness degradation.

The repair was capable of restoring the degraded performance of the specimens in terms of lateral displacement, lateral load, energy dissipation and stiffness.

The important components of the repair method were a CFRP shell, post-installed headed steel bars and concrete inside the CFRP shell. The CFRP shell provided confinement, shear strength and hoop tension. The post-installed headed bars were successful in providing sufficient flexural capacity to relocate the plastic hinge; they provided a means to transfer the tension lost by the fractured original column longitudinal bars connecting the columns to the footing or pier cap.

Both nonshrink and expansive concrete were successful in restoring the capacity of the column. The nonshrink concrete in the CFRP shell provided sufficient passive confinement. The expansive concrete in the CFRP shell provided active confinement. The use of expansive instead of nonshrink concrete caused sufficient expansion to produce an active confinement system. However, control of the amount of concrete expansion is important as excessive initial expansion will reduce the remaining tensile capacity of the CFRP shell.

Based on the overall performance of the repaired specimens this is a viable technique for damaged precast RC columns in seismic regions. In the present case, the initial damage of the precast RC columns was severe therefore the repair method is robust and would be applicable to precast RC columns with varying damage states. The repair technique can be installed in approximately one week which is advantageous in emergency response situations and is an excellent application for accelerated bridge repairs.

REFERENCES

1. Seible, F.; Priestley, M.; Hegemier, G.; and Innamorato D., 1997. “Seismic Retrofit of RC Columns with Continuous Carbon Fiber Jackets.” Journal of Composites for Construction, V.1, No. 2, 52-62.
2. Saadatmanesh, H.; Ehsani. M.; and Jin, L., 1997. ‘‘Repair of Earthquake-damaged RC Columns with FRP Wraps.’’ ACI Structural Journal, V.94, No. 2, 206–215.
3. Gergely, I.; Pantelides, C.; Nuismer, R.; and Reaveley, L., 1998. “Bridge Pier Retrofit using Fiber-reinforced Plastic Composites.’’ Journal of Composites for Construction, V. 2, No. 4, 165–174.
4. Xiao, Y.; Wu, H.; and Martin, G. R., 1999. “‘Prefabricated Composite Jacketing of RC Columns for Enhanced Shear Strength.’’ Journal of Structural Engineering, V. 125, No. 3, 255–264.
5. Pantelides, C.; Gergely, J.; Reaveley, L.; and Volnyy, V., 1999. ‘‘Retrofit of RC Bridge Pier with CFRP Advanced Composites.’’ Journal of Structural Engineering, V. 125, No. 10, 1094–1099.
6. Pantelides, C.; Alameddine, F.; Sardo, T.; and Imbsen, R., 2004. ‘‘Seismic Retrofit of State Street Bridge on Interstate 80.’’ Journal of Bridge Engineering, V. 9, No. 4, 333–342.
7.Chai, Y.; Priestley, N.; Seible, F., 1991. “Seismic Retrofit of Circular Bridge Columns for Enhanced Flexural Performance. ACI Structural Journal. Vol. 88, No. 5, 572-584.

8. Priestley, N.; Seible, F.; Xiao, Y.; and Verma, R., 1994. "Steel Jacket Retrofitting of RC Bridge Columns for Enhanced Shear Strength. Part 2: Test Results and Comparison with Theory." ACI Structural Journal, V. 91, No. 5, 537-551.
9. Xiao, Y.; and Wu, H., 2003. "Retrofit of RC Columns using Partially Stiffened Steel Jackets." Journal of Structural Engineering, V. 129, No. 6, 725-732.
10. Rodriguez, M.; and Park, R., 1994. "Seismic load tests on RC columns Strengthened by Jacketing." ACI Structural Journal. Vol. 91, No.2, 150-159.
11. Lehman, D.; Gookin, S.; Nacamuli, A.; and Moehle J., 2001. "Repair of earthquake-damaged bridge columns." ACI Structural Journal; 98 (2): 233-242.
12. Rutledge, S.T.; Kowalsky, M.J.; Seracino, R.; and Nau, J.M., 2014. "Repair of RC bridge columns containing buckled and fractured reinforcement by plastic hinge relocation." Journal of Bridge Engineering; Vol. 19(8), A4013001.
13. Haber, Z.B.; Saiidi, M.S.; and Sanders, D.H., 2014. "Seismic Performance of Precast Columns with Mechanically Spliced Column-footing Connections." ACI Structural Journal; Vol. 111, No. 3; 639-650.
14. Ameli, M.J; Parks, J.E.; Brown, D.N.; Pantelides, C.P.; Sletten, J.; and Swanwick, C., 2013. "Seismic evaluation of grouted splice sleeve connections for precast reinforced concrete bridge piers." Proceedings of the 7th National Seismic Conference on Bridges & Highways; Paper No. A3-5. Oakland, California.
15. Ameli, M.J; Parks, J.E.; Brown, D.N.; Pantelides, C.P.,2015."Seismic Evaluation of Grouted Splice Sleeve Connections for Reinforced Precast Concrete Column-to-Cap Beam Joints in Accelerated Bridge Construction." Journal of the Precast/Prestressed Concrete Institute; Vol. 60, No. 2; 80-103.
16. Tazarv, M.; Saiidi, M.S, 2014. "Next Generation of Bridge Columns For Accelerated Bridge Construction in High Seismic Zones." California Department of Transportation.; Report No. CA14-2176.
17. Pantelides, C.P.; Ameli, M. J.; Parks, J.E.; and Brown, D.N., 2014. "Seismic Evaluation of Grouted Splice Sleeve Connections for Precast RC Bridge Piers in ABC." Utah Department of Transportation Research Division; Report No. UT-14.09.
18. Yan, Z.; Pantelides, C.P; and Reaveley, L.D., 2006. "Fiber-reinforced Polymer Jacketed and Shape-modified Compression Members: 1- Experimental Behavior." ACI Structural Journal; Vol. 103, No. 6; 226-234.
19. American Association of State Highway and Transportation Officials, 2011. "AASHTO Guide Specifications for LRFD Seismic Bridge Design." AASHTO ; 2nd edition.
20. ACI Committee 374. Guide for testing reinforced concrete structural elements under slowly applied simulated seismic loads. ACI 2013; ACI 374.2R-13, Farmington Hills, MI.
21. Hose, Y.; Seible, F., 1999."Performance Evaluation Database for Concrete Bridge Components and Systems under Simulated Seismic Loads." Pacific Earthquake Engineering Research Center.
22. Brown, D.N., 2014, "Post-earthquake repair of precast concrete column-to-footing plastic hinges," MS Thesis, Univ. of Utah, Salt Lake City, UT.
23. Parks, J.E., 2014, "Seismic Rehabilitation of column to pier cap ABC connections and AE monitoring assessment," MS Thesis, Univ. of Utah, Salt Lake City, UT.
24. Moran D, Pantelides C. Elliptical and circular FRP-confined concrete sections: a Mohr-Coulomb analytical model. International Journal of Solids and Structures 2012; 49: 881-898.

25. ASTM Standard D3039. "Standard test method for tensile properties of polymer matrix composite materials". ASTM International, PA, 2014.www.astm.org.
26. American Concrete Institute Committee 440, 2008, "ACI 440.2R-08 Guide for the Design and Construction of Externally Bonded FRP Systems for Strengthening Concrete Structures," Farmington Hills, MI.